Chemical Physics Letters 503 (2011) 262–265

Contents lists available at ScienceDirect

Chemical Physics Letters

journal homepage: www.elsevier.com/locate/cplett

Efficient photocatalytic hydrogen production over Ni@C/TiO_2 nanocomposite under visible light irradiation

Peng Zeng, Xungao Zhang *, Xiaohu Zhang, Bo Chai, Tianyou Peng *

College of Chemistry and Molecular Science, Wuhan University, Wuhan 430072, China

ARTICLE INFO

Article history:
Received 27 November 2010
In final form 3 January 2011
Available online 6 January 2011

ABSTRACT

A novel visible-light-driven carbon-coated Ni (Ni@C)/TiO_2 nanocomposite photocatalyst with enhanced photoactivity for hydrogen production was synthesized and characterized for the first time. The resultant Ni@C/TiO_2 nanocomposites are composed of nanorods with an average diameter of ca. 10 nm and length in the range of 40–100 nm, and exhibit remarkable photostability in an aqueous suspension by using triethanolamine (TEOA) as a sacrificial reagent. Moreover, a hydrogen generation rate of up to 300 μmol h^{-1} over 5 wt% Ni@C/TiO_2 without Pt-loading is achieved under visible light ($\lambda \geqslant 420$ nm) irradiation.

1. Introduction

As a chemical stable, environmentally friendly, abundant and cost effective photocatalyst, titania (TiO_2) can only absorb UV light with low quantum efficiency due to its wide energy-gap (ca. 3.2 eV), which limits its photocatalytic H_2 production application. Therefore, the development of visible-light-driven photocatalysts has received much attention due to its potential applications of a hydrogen energy conversion system from solar energy [1,2]. Moreover, various noble metal species such as Pt and RuO_2 have been used in most cases as cocatalysts to promote H_2 production by reducing the over-potential loss [3,4], but many meaningful endeavours have focused on developing photocatalysts with non-noble metals (e.g. Ni) as cocatalyst [5,6].

Recently, both steady visible-light-driven photoactivity and enhanced H_2 production efficiency over Pt-loaded multiwalled carbon nanotubes (MWCNTs)/TiO_2 nanocomposites have been achieved in our group [7]. MWCNTs in the nanocomposite can make TiO_2 respondent also to visible light region, but it is still necessary to load noble metal Pt as H_2 evolution promoter. Our previous researches have shown especially chemical and thermal stability when ferromagnetic metal (such as Fe, Co and Ni) was coated with carbon [8], these carbon-coated ferromagnetic metal (denoted as metal@C) materials have been used as high-density magnetic recording media, magnetically separable catalysts and biomedical applications for years [9–11]. It is reasonable to expect that Ni@C/TiO_2 nanocomposite photocatalyst would enhance the visible light response and photocatalytic activity for H_2 production due to the synergistic effect of suppression of the recombination of photogenerated carriers and photosensitization just like the above-mentioned MWCNTs/TiO_2, and the carbon-coated Ni nanocrystallites can act as cocatalyst [5,6], whereas less work has been done on the photocatalytic H_2 production, which is thought to be one of the best approaches for obtaining clean and sustainable energy [1–4]. To the best of our knowledge, for the first time in this Letter we employed a facile hydrothermal process to fabricate a novel nanocomposite containing TiO_2 and Ni@C *in situ* through a surfactant-mediated templating route [7,12]. The obtained Ni@C/TiO_2 nanocomposite was used as photocatalyst for H_2 production in triethanolamine (TEOA) solution under visible-light irradiation, and the effect of Ni@C on the efficiency of photocatalytic H_2 evolution over the nanocomposites was studied in detail.

2. Experimental details

2.1. Material preparation

Ni@C was prepared by an AC arc discharge method under He gas atmosphere according to our previous publication (ESI, Figure S1) [8], and pretreated by 2 M HCl solution in order to remove the uncoated Ni. The Ni@C contains 67.9 wt% cubic Ni nanocrystallites, which is encapsulated by graphite-like carbon, with particle sizes in the range of 10–50 nm [8]. Ni@C/TiO_2 containing various Ni@C contents were hydrothermally prepared through a cetyltrimethylammonium bromide (CTAB)/$Ti(SO_4)_2$ system, similar to our previous processes [7,12] except that the initial pH value was adjusted to 8.0 by ammonia.

2.2. Material characterization

X-ray powder diffraction (XRD) patterns of Ni@C/TiO_2 were obtained on a Bruker D8 advance X-ray diffractometer with a Cu-Kα

---

* Corresponding authors. Fax: +86 27 6875 2237.
E-mail addresses: xgzhang66@whu.edu.cn (X. Zhang), typeng@whu.edu.cn (T. Peng).

0009-2614/$ - see front matter © 2011 Elsevier B.V. All rights reserved.
doi:10.1016/j.cplett.2011.01.007

radiation at 40 kV and 100 mA. Field emission scanning electron microscopy (FESEM) images were obtained on a JSM-7400F electron microscope. Transmission electron microscopy (TEM) images were obtained on a LaB6 JEM-2010(HT)-FEF electron microscope. X-ray photoelectron spectra (XPS) were recorded on a Kratos ASIS-HS X-ray photoelectron spectroscope equipped with a standard and monochromatic source (Al-Kα) operated at 150 W (15 kV, 10 mA). The UV–Vis diffuse reflectance absorption spectra (DRS) were recorded by a Cary 5000 UV–Vis-NIR spectrophotometer equipped with an integrating sphere. The carbon and nickel element contents were detected by using Bruker S4 Pioneer X-ray fluorescence (XRF) spectrometer in a standardless mode.

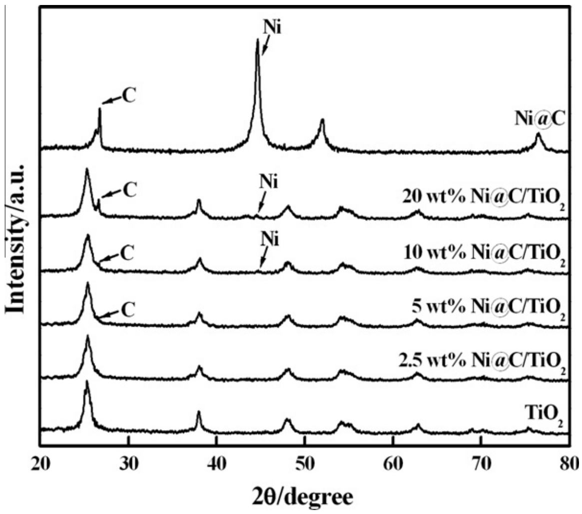

Figure 1. XRD patterns of Ni@C/TiO_2 nanocomposites containing different Ni@C contents.

2.3. Photocatalytic activity evaluation

Photocatalytic reactions were carried out in an outer irradiation-type photoreactor (Pyrex) connected a closed gas-circulation system. A 300 W Xe-lamp (PLS-SXE300, Beijing Trusttech Co., China) equipped with a cutoff filter (Kenko L-42, $\lambda \geqslant 420$ nm) was applied as the light source. The photocatalytic reaction was performed in 100 mL water suspension containing 15 vol% triethanolamine (TEOA) and photocatalyst (150 mg). Then the suspension was thoroughly degassed to remove air, and irradiated from the top of the reactor system. The photocatalytic H_2 evolution rate was determined by using SP-6800A gas chromatograph (TCD detector, 5 Å molecular sieve columns and Ar carrier).

3. Results and discussion

3.1. XRD result analyses

Figure 1 shows the XRD patterns of Ni@C/TiO_2 nanocomposites containing different Ni@C contents. The main diffraction peaks of various products can be ascribed to anatase TiO_2, while the peaks at $2\theta = 26.5°$ for the graphite-like carbon can also be detected once the Ni@C content is more than 5 wt%. When the Ni@C content is larger than 10 wt%, metal Ni species can be seen from the XRD pattern, and those nanocomposites with Ni@C content lower than 10 wt% do not show the relative Ni diffraction peaks, implying that part Ni might be oxidized and/or lost during the preparation process. This assumption can be further validated by the XRF analysis results (ESI, Table S1), in which Ni content in various nanocomposites is slightly lower than its addition amount.

3.2. Morphology and component analyses

Figure 2a and b shows the FESEM images of the pristine TiO_2 and 5 wt% Ni@C/TiO_2. It is noteworthy that the pristine TiO_2 derived from the present experiment condition shows nanorod-like

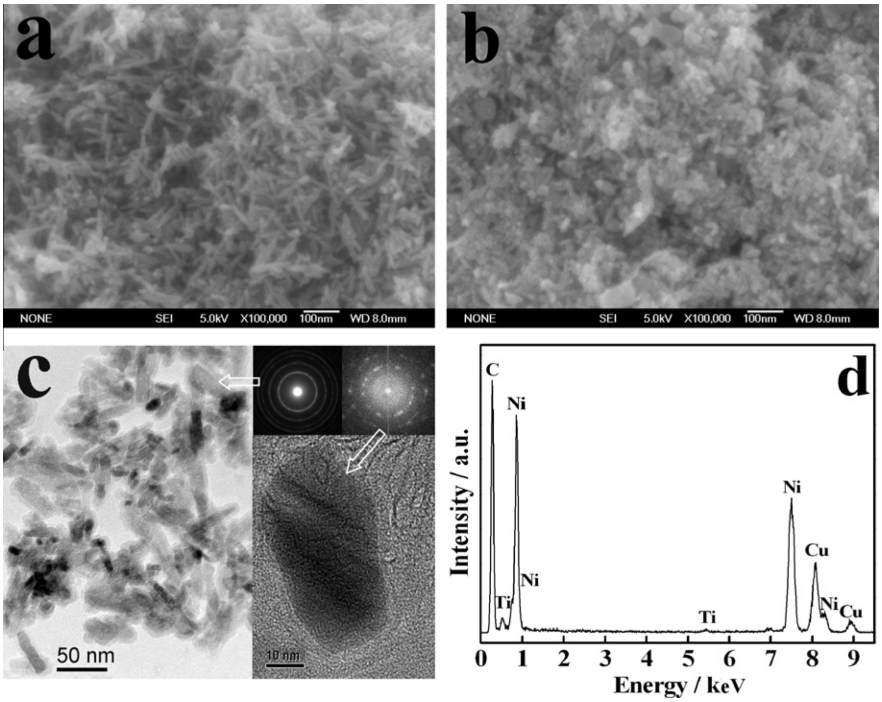

Figure 2. FESEM and TEM images of various products. a: Pristine TiO_2; b and c: 5 wt% Ni@C/TiO_2; d: EDX spectrum of 5 wt% Ni@C/TiO_2.

morphologies with average diameter of ca. 10 nm and length in the range of 40–120 nm (Figure 2a). After addition of 5 wt% Ni@C, the nanocomposite shows shorter nanorod-like structures co-existing with large amount of nanoparticles (Figure 2b), indicating addition of Ni@C can retard the formation of nanorod-like TiO_2 during the hydrothermal process. TEM images can offer further insight into the morphology and microstructure of Ni@C/TiO_2. As can be seen from Figure 2c, the obtained nanocomposite shows nanorod-like structures coexisting with nanoparticles as observed from Figure 2b. The inserted selected area electron diffraction (SEAD) pattern taken from Figure 2c reveals the multicrystalline feature of TiO_2. The HRTEM image inserted in Figure 2c shows that most Ni@C microstructures are maintained during the present conditions, and the Fast Fourier Transform (FFT) pattern for the Ni@C indicates the sample containing metal Ni species. The energy dispersive X-ray (EDX) spectrum in Figure 2d also indicates there are obviously C and Ni elements in the nanocomposite.

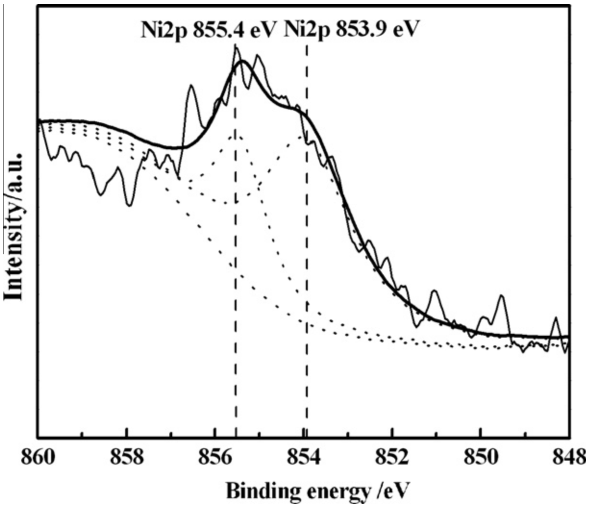

Figure 3. XPS spectrum for Ni 2p of 20 wt% Ni@C/TiO_2 nanocomposite.

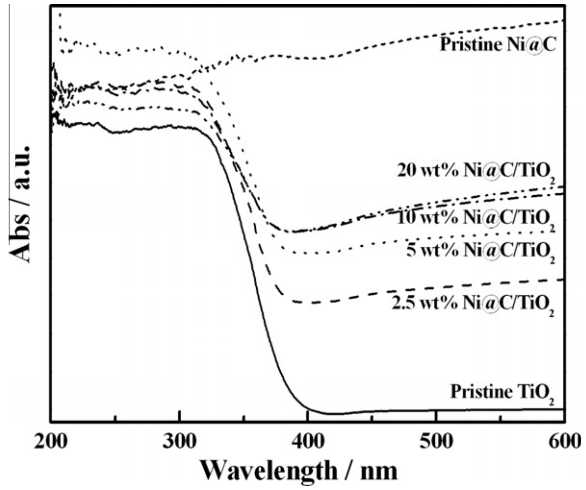

Figure 4. UV–Vis diffuse reflectance absorption spectra (DRS) of Ni@C/TiO_2 nanocomposites containing different Ni@C contents.

XPS can supply some proofs of above suggestions (ESI, Figure S2). There is no obvious XPS peak due to Ni species observed from 5 wt% Ni@C/TiO_2, implying that most Ni species are enveloped by the graphite-like carbon and maintained its original structure. Even for 20 wt% Ni@C/TiO_2, XPS pattern of Ni species is quite indistinct as shown in Figure 3. The XPS peaks of 853.9 eV and 855.4 eV may be assigned to NiO and Ni_2O_3, respectively. Possibly, NiO_x as cocatalysts can promote the H_2 production as reported in previous literatures [13–15]. Based on above observations, it is reasonable to conjecture that most Ni@C maintained its original structures, whereas small part Ni@C changed into metal oxide clusters highly dispersed on TiO_2 during the preparation procedure.

3.3. Absorption spectra analyses

Figure 4 shows the UV–Vis diffuse reflectance absorption spectra (DRS) of Ni@C/TiO_2 nanocomposites containing different Ni@C contents. Upon enhancing the Ni@C content, the absorption intensity of the nanocomposite gradually increases, plausibly due to the color changed to darker. It can be observed that introducing Ni@C to TiO_2 could enhance the visible light absorption ability of the nanocomposite with extended absorption tail into the whole range of visible light region. This absorption enhancement at wavelengths greater than 400 nm would have an influence on the fundamental process of formation of electron/hole pairs and their separation in the photocatalytic process under light illumination [7].

3.4. Photocatalytic activity and stability

The photoactivities for H_2 evolution from an aqueous suspension containing TEOA and Ni@C/TiO_2 with different Ni@C contents are achieved under visible-light irradiation. Effects of Ni@C content and photocatalyst addition amount are also investigated (ESI, Figures S3 and S4). The maximum photocatalytic H_2 evolution efficiency is obtained from 5 wt% Ni@C/TiO_2 suspension (150 mg). It is possible that this nanocomposite achieved the optimum light absorption capability and photogenerated carriers' separation efficiency [7]. Further experiments show that the pristine Ni@C and the physical mixture of 5 wt% Ni@C and TiO_2 also exhibits detectable photoactivity for H_2 production; whereas the hydrothermally prepared nanocomposites containing TiO_2 and single soot (amorphous carbon, prepared by an AC arc discharge under the same conditions of Ni@C without addition of Ni power) or Ni powders (instead of Ni@C) show no detectable photocatalytic H_2 production as shown in Table 1. Even the mixture of soot and Ni powders with the same content as Ni@C is introduced into the hydrothermal reaction system, the as-made product still shows no obvious photoactivity. However, 5 wt% Ni@C/TiO_2 shows the highest H_2 evolution efficiency among all above products. Therefore, it can be conjectured that the graphite-like carbon could act as photosensitizer, similar to the MWCNTs absorbing the visible light, which

Table 1
Photocatalytic H_2 evolution activities of various products under visible-light irradiation.

Photocatalysts	Soot/TiO_2[a]	Ni/TiO_2[b]	Ni@C	(Soot + Ni)/TiO_2[c]	5 wt%Ni@C/TiO_2	5 wt%Ni@C + TiO_2[d]
H_2 evolution/μmol h^{-1}	0	0	21.5	0	300	34.4

Photocatalytic conditions: 100 mL aqueous suspension containing 15 vol% TEOA and 150 mg catalyst, $\lambda \geqslant 420$ nm light irradiation 5 h.

[a] Soot was prepared by an AC arc discharge process under the same conditions as Ni@C without addition of Ni power.

[b] Ni/TiO_2 was prepared by using Ni powder instead of Ni@C.

[c] Soot and Ni powder with the same content as Ni@C were introduced into the hydrothermal system.

[d] Physical mixture of 5 wt% Ni@C and TiO_2, and TiO_2 was prepared under the same hydrothermal conditions without addition of Ni@C.

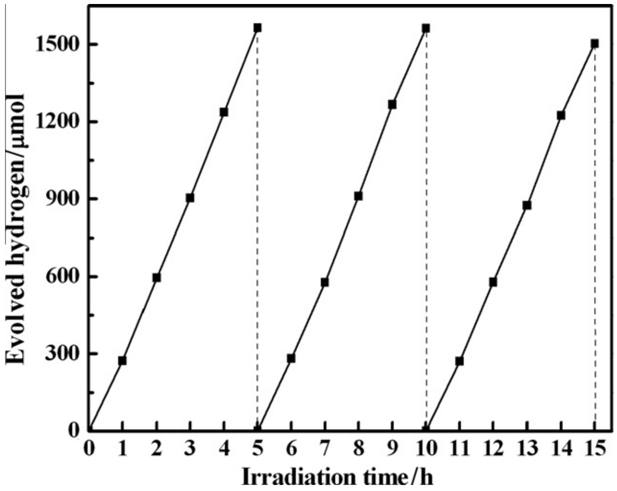

Figure 5. Time course of the photocatalytic H_2 production from 100 mL aqueous suspension containing TEOA (15 vol%) and 5 wt% Ni@C/TiO_2 (150 mg) under visible light ($\lambda \geqslant 420$ nm) irradiation.

can inject the photogenerated electrons into TiO_2 conduction band as mentioned in our previous paper [7]. Meanwhile, the synergetic effect of the intrinsic properties of components in the present nanocomposite is also beneficial for the electron transfer in the conduction band to reduce the water molecules for H_2 production [7,16,17].

Figure 5 shows the time course of photocatalytic H_2 production over 5 wt% Ni@C/TiO_2. As can be seen, a steady visible-light-driven photoactivity and enhanced H_2 production efficiency over Ni@C/TiO_2 are both achieved, and more than 4500 μmol of H_2 was obtained during 15 h photoreaction with H_2 production efficiency of 300 μmol h^{-1}, whereas the pristine Ni@C only produced about 21.5 μmol h^{-1}. Moreover, the photoactivities for H_2 production over 5 wt% Ni@C/TiO_2 and pristine Ni@C upon incident monochromatic light wavelength are also investigated. Both of the photocatalysts show a wide photoresponse under monochromatic light wavelength ranged from 350 to 550 nm. Ni@C/TiO_2 demonstrates high apparent quantum efficiency (AQE) calculated according to the previous literature [18]. The AQE under 420 and 520 nm monochromatic light irradiation is 12% and 7%, respectively. It is much higher than the relative AQE values (3% and 2%) of Ni@C at 420 and 520 nm. Production of H_2 is also observed when methanol was used instead of TEOA, although the hydrogen evolution rate was lower.

The dramatically enhanced H_2 production efficiency of the nanocomposites can be mainly ascribed to the synergetic effect of the intrinsic properties of its components such as an excellent light absorption and charge separation on the interfaces between the Ni@C and TiO_2 derived from the hydrothermal process, though we do not clearly understand it till now. The above experimental facts suggest a promising strategy to develop efficient and stable photocatalyst for H_2 production.

4. Conclusion

A novel Ni@C/TiO_2 nanocomposite was successfully synthesized via a hydrothermal treatment. The experimental results demonstrate addition of Ni@C benefits the enhancement of visible light adsorption and photogenerated carrier separation. Steady visible-light-driven photoactivity and enhanced H_2 production efficiency were both achieved from the present nanocomposite. These results suggested interesting possibilities for the preparation of more efficient panchromatic photocatalysts with better durability and more broader light absorption range (e.g. including UV light) in comparison with the organic dye-sensitized semiconductors, which usually cannot survive from the UV light illumination. Thus, as a novel and stable artificial visible-light-driven photocatalyst for H_2 production, Ni@C/TiO_2 seems to suggest a way in making panchromatic respondent and low-cost (without noble metal-loading) photocatalysts. Future investigation on its systematic characterization and photocatalytic mechanism is under progress.

Acknowledgments

This work was supported by the NSFC (20973128), Program for New Century Excellent Talents in University (NCET-07-0637), and Independence Innovation Program (2081003) of Wuhan University, China.

Appendix A. Supplementary data

Electronic Supplementary Information (ESI): details of Preparation procedures and photocatalytic reaction condition optimization for the Ni@C/TiO_2 nanocomposite. Supplementary data associated with this article can be found, in the online version, at doi:10.1016/j.cplett.2011.01.007.

References

[1] Z.G. Zou, J.H. Ye, K. Sayama, H. Arakawa, Nature 414 (2001) 625.
[2] X.B. Chen, S.H. Shen, L.J. Guo, S.S. Mao, Chem. Rev. 110 (2010) 6503.
[3] M.Y. Liu et al., Chem. Commun. (2004) 2192.
[4] J. Sato et al., J. Am. Chem. Soc. 127 (2005) 4150.
[5] A. Kudo, M. Sekizawa, Chem. Commun. (2000) 1371.
[6] D.H. Kim, H.S. Park, S.J. Kim, K.S. Lee, Catal. Lett. 100 (2005) 49.
[7] K. Dai, T.Y. Peng, D.N. Ke, B.Q. Wei, Nanotechnology 20 (2009) 125603.
[8] J. Ling, Y. Liu, G.M. Hao, X.G. Zhang, Mater. Sci. Eng. B 100 (2003) 186.
[9] K. Hayashi, M. Ohsugi, M. Kamigaki, B. Xia, K. Okuyama, Electrochem. Solid St. 5 (2002) J9.
[10] S.C. Tsang, V. Caps, I. Paraskevas, D. Chadwick, D. Thompsett, Angew. Chem. Int. Ed. 43 (2004) 5645.
[11] A. Arrais et al., Chem. Commun. (2008) 5936.
[12] T.Y. Peng, D. Zhao, K. Dai, W. Shi, K. Hirao, J. Phys. Chem. B 109 (2005) 4947.
[13] H. Kato, A. Kudo, J. Phys. Chem. B 105 (2001) 4285.
[14] H. Kato, K. Asakura, A. Kudo, J. Am. Chem. Soc. 125 (2003) 3082.
[15] M. Tian, W.F. Shangguan, J. Yuan, S.J. Wang, Z. Ouyang, Sci. Technol. Adv. Mater. 8 (2007) 82.
[16] W.D. Wang, P. Serp, P. Kalck, J.L. Faria, J. Mol. Catal. A-Chem. 235 (2005) 194.
[17] Y. Ou, J.D. Lin, S.M. Fang, D.W. Liao, Chem. Phys. Lett. 429 (2006) 199.
[18] A. Kudo, Y. Miseki, Chem. Soc. Rev. 38 (2009) 253.